Geol. Mag. **134** (*4*), *1997, pp. 557–561. Printed in the United Kingdom* *© 1997 Cambridge University Press*

Unidirectional to bidirectional subtidal sandwaves influenced by gradually decreasing steady flow velocity

KATSUHIRO NAKAYAMA

Department of Geoscience, Shimane University, Nishikawatsu, Matsue 690, Japan

(*Received* 12 Februaury 1997; *accepted* 12 May 1997)

Abstract

Miocene subtidal sandwave deposits in southwest Japan were influenced by periodic flow and steady flow. The sandwave deposits can be divided into five units, based on lithofacies and thickness. In order of accretion, unit 1 consists of unidirectional sand bedforms without mud drapes, unit 2 of unidirectional sand bedforms with thin, discontinuous mud drapes, unit 3 of bidirectional sand bedforms with thin continuous mud drapes, and units 4 and 5 of relatively thinner and smaller bidirectional sand bedforms with continuous mud drapes. The thickness of units 1 to 3 increase progressively to 2.6 m, and units 4 to 5 subsequently decrease from 2.0 to 1.0 m. Variations between the units are due to differing combinations of periodic and steady flow velocities. Palaeoflow velocity is estimated from grain size and unit thickness. Depth-mean velocities of steady flow components gradually decrease from 0.72 m s^{-1} to 0.16 m s^{-1} with unit accumulation.

1. Introduction

Tide-dominated stratigraphic records are important because they can provide many parameters of physical palaeomarine conditions. The sequence stratigraphy concept has further emphasized their importance in connection with sea-level changes (Walker, 1992). Many examples of modern and ancient tide-dominated deposits have been described in the past ten years (e.g. de Boer, van Gelder & Nio, 1988). Tidal sandwave deposits, which are representative tide-dominated deposits, have been widely recognized in modern shallow water tidal environments (Dalrymple, 1984), and several have been described from the stratigraphic records (e.g. Allen & Homewood, 1984; Murakoshi, Nakayama & Masuda, 1995). Depositional models for tidal sandwaves are explained by combinations of periodic and steady flows (Allen, 1980). It is fair to say, however, that stratigraphic records of subtidal sandwaves influenced by steady flow are very rare, compared with those of modern tidal sandwaves which have been influenced by fluvial steady flow (e.g. Coleman & Wright, 1975; Gastaldo, Allen & Huc, 1995), and other tidal sandwave deposits in stratigraphic records.

2. Geological outline

The sandwave deposits discussed here occur in the Miocene Matsue Formation in southwest Japan. The Matsue Formation, deposited in the back-arc basin of the Japan Sea, is composed mainly of sandstone and mudstone beds, with intercalated alkalic basalt lava flow beds. K–Ar radiometric ages of these lava beds indicate between 10.7 and 11.9 Ma (Kano & Nakano, 1985; Morris *et al.* 1990). Outcrops in two cliffs at the locality point indicate upward-shallowing from bay to swamp margin environments, because wood fragments and roots increase in abundance towards the top of the successions. The sandwave deposits occur within intensely bioturbated mudstone to muddy sandstone successions in the eastern cliff (Fig. 1). According to geochemical analysis, the entire successions in the outcrops contain more than 3 wt% sulphur as pyrite (Nakayama *et al.* 1996), suggesting a subtidal environment (Berner, 1984) as opposed to inter- or supra-tidal. Roots of swamp vegetation can penetrate several metres below the surface of subtidal mudflats, based on the recent vegetation study on salt marsh and swamp areas (Suzuki, Takeda & Kurihara, 1988). Abundance of roots in the upper part of the succession thus supports a very shallow subtidal environment. According to the ratio of organic carbon to nitrogen of ~30 (Hedges, Clark & Cowie, 1988), organic carbon in the sediments originated from terrigenous plant fragments (Nakayama *et al.* 1996). Palaeogeographically, emergent land was present less than 2 km to the south of the outcrop during deposition (Kano *et al.* 1994).

3. Description of the sandwave deposits

The sandwave deposits show concave-up erosional bases, and thin out in the southern margin of the outcrop. From the genetic viewpoint, the term sandwave is used here in the sense of Allen (1980), however, bedform terminology follows Ashley (1990). Proportions of mud in the sandwave deposits generally increase with order of deposition. The sandwave deposits consist mainly of dune foresets with banded mud drape layers, associated with ripples. Biogenetic burrows (*Psilonichus* and others) occasionally disturb laminations (Fig. 3). Almost all dune foresets dip northeast at 10° to 20°, although a few exceptional dune foresets dip south-southwest (Figs. 2 and 3). Each foreset dune layer is almost less than 10 cm thick. Reworked shell and wood fragments are frequently founded at the base of the foresets. Ripples occur as lenticular to wavy beddings (Reineck & Wunderlich, 1968). Current ripples, and combined wave and current ripples, are found with palaeoflow directions mainly towards the south-southwest and the northeast (Fig. 2). Mud drape layers vary from 1 mm to 4 cm in thickness. However, mud layers thicker than 4 mm also include very thin and discontinuous intercalated sand laminae.

The sandwave deposits comprise five units, numbered unit 1 to 5 in order of accretion. Each unit is separated by an erosional surface. Unit 1 consists only of dune foreset sandstones, while unit 2 comprises dune foreset and ripple sandstones and discontinuous thin mud drape layers. Dune foreset sandstones of both units and ripple sandstones of unit 2 dip northeast, and no bed-

https://doi.org/10.1017/S0016756897007450 Published online by Cambridge University Press

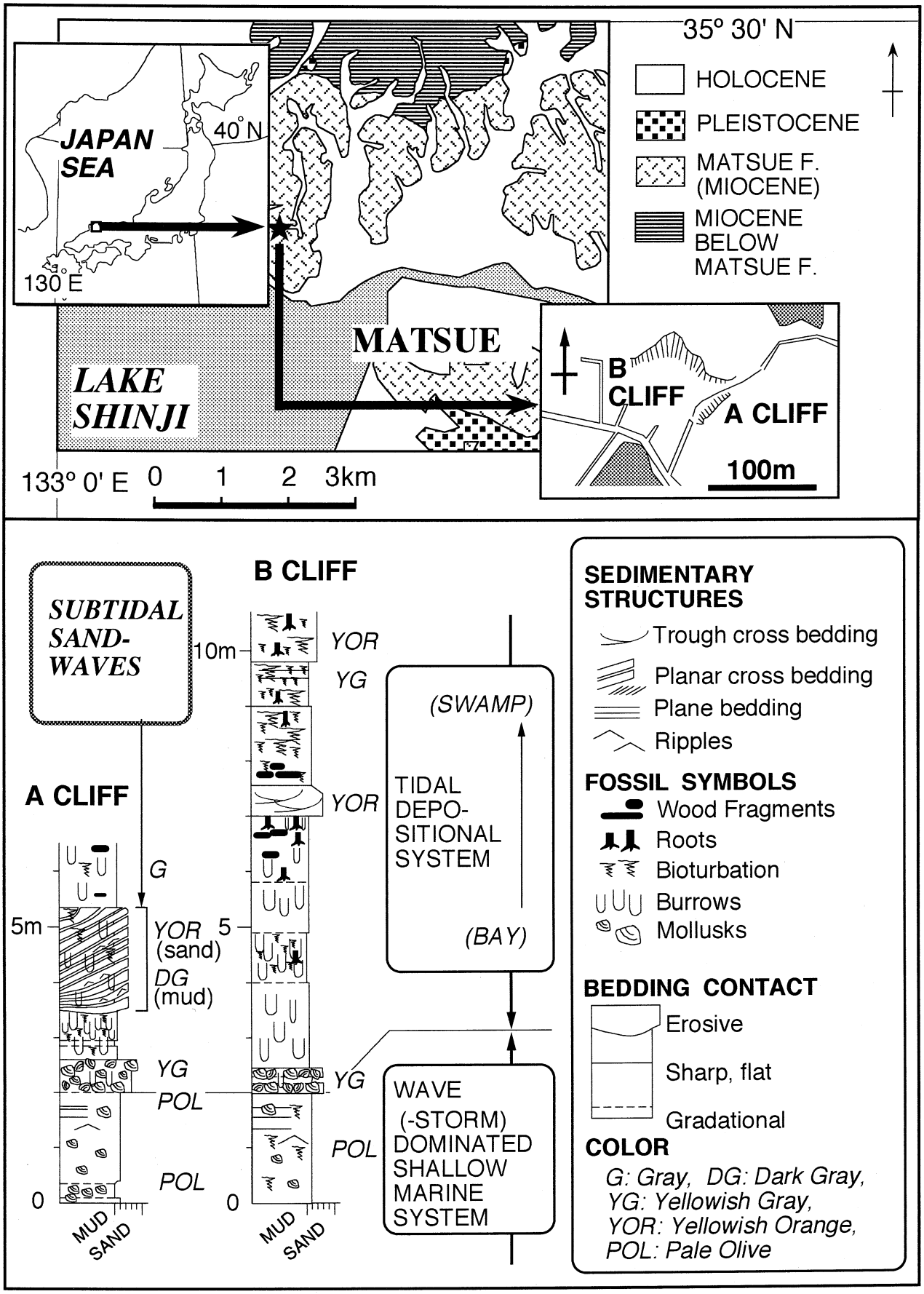


Figure 1. Map of the study area showing the location at Matsue in southwest Japan, and graphic log sections (after Nakayama *et al.* 1996).

https://doi.org/10.1017/S0016756897007450 Published online by Cambridge University Press

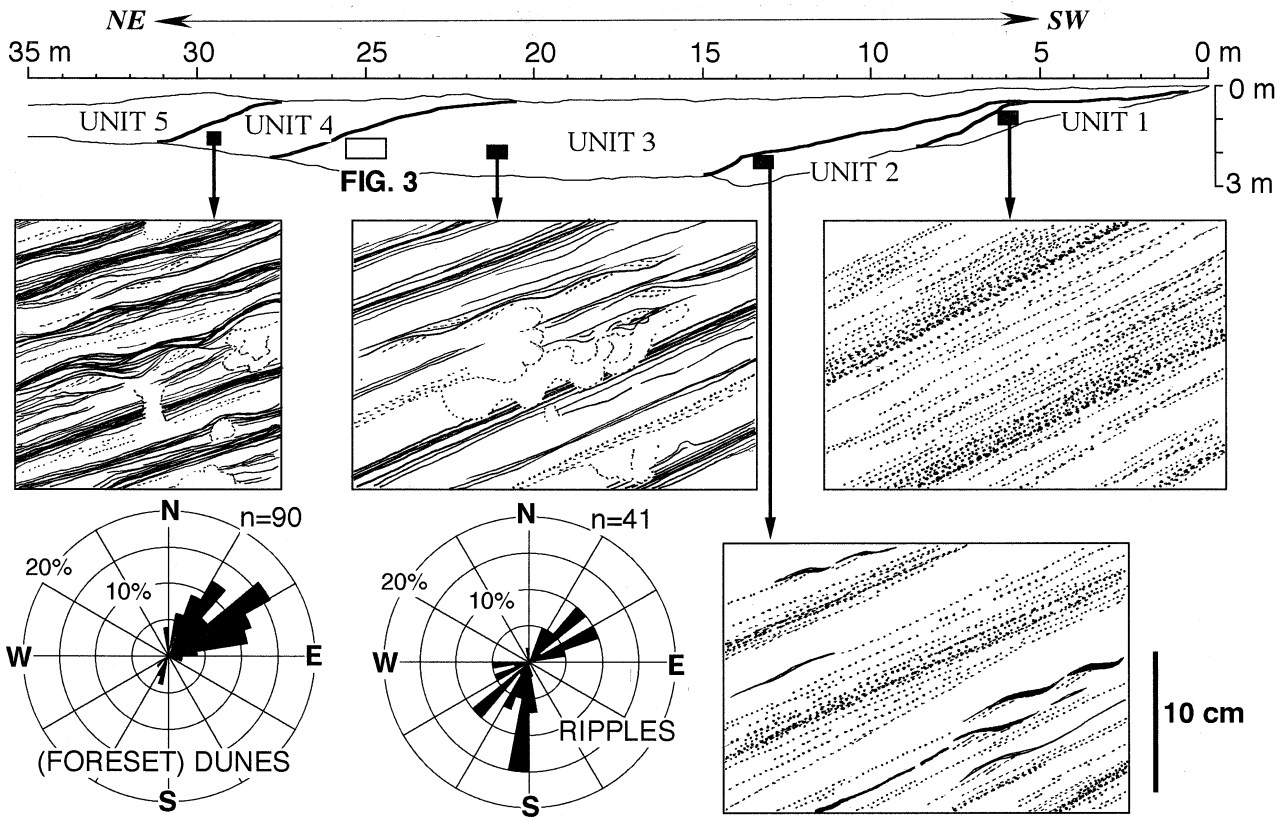


Figure 2. Sketch of the subtidal sandwave deposits (at A cliff in Fig. 1) in the Miocene Matsue Formation. Detailed sketches are the same scale. Dotted lines are sand forming laminations, solid lines are mud drape layers. Some laminae are biogenetically disturbed. Rose diagrams indicate the azimuths of foreset dunes and ripples. South-southwest-directed dunes are measured in the exceptional subunit of unit 3.

forms showing palaeoflow toward the south-southwest are observed. Discontinuous drape layers are well preserved on the stoss side of ripples. Unit 3 is accreted on both units 1 and 2 with an apparent erosional surface. Unit 3 is generally composed of northeast-dipping dune foreset sandstones, continuous mud drape layers, and ripple sandstones. Palaeoflow direction of the ripples is predominantly toward the south-southwest. In unit 3, one subunit is superimposed, 24 m to 26 m from the southern margin of the sandwave deposits. This subunit comprises south-southwest-dipping foreset dunes and mud drapes, which are tidal rhythmites (Dalrymple, Makino & Zaitlin, 1991) reflecting neap–spring cycles (Fig. 3). Mud drapes in the subunit occur as mud layer couplets (Visser, 1980). Units 4 and 5 consist of continuous mud drape layers and sand bedforms. Sand bedforms in these units are relatively thin (2–3 cm) dune

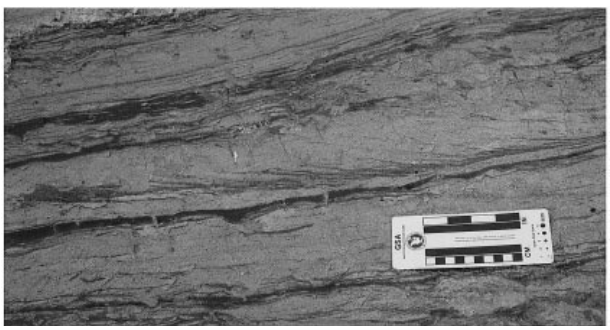


Figure 3. One bundle set in the subunit of unit 3. Thin bundles in left (1 to 7 mm in bundle thickness) correspond to tides around neap tide; thick bundles in right (10 to 15 mm in bundle thickness) correspond to tides around spring tide.

foresets and ripples. In places in the bottom parts of these units, lenticular to wavy ripples show alternate palaeoflow direction. Unit 4 decreases in thickness from 2.0 to 1.6 m in order of accretion. Unit 5, 1.6 to 1.0 m in thickness, is accreted onto unit 4.

4. Interpretation of the sandwave deposits

The sandwave deposits can be explained as subtidal sandwaves influenced by both periodic and steady flows. Mud layer couplets in the sandwave deposits indicate a subtidal environment (Visser, 1980), which is supported by the occurrence of pyrite. Periodic flow in shallow marine settings is typically reflected by tidal cycle. In contrast, there are several possibilities for steady flow origin, including fluvial currents, thermohaline currents, wind drift currents and atmospheric pressure-formed currents (Allen, 1982). However, considering the close proximity of emergent land to the south, and the abundance of organic carbon of terrigenous plant origin, the steady flow in these sandwave deposits could have originated from fluvial currents. Fluvial current as steady flow is still one possibility. On the other hand, the palaeogeographic setting suggests that palaeoflow toward the northeast is the ebb direction, and that toward the south-southwest is the flood direction. The ebb-directed current is generally the dominant current in these sandwave deposits. The lithofacies differences between each unit are thought to be formed by periodic flow of tidal origin, combined with decreasing steady flow velocity (Fig. 4). Unit 1 comprises northeast-dipping dune foreset sandstones without mud drapes, and is lacking bedforms toward the south-southwest, suggesting deposition from strong steady flow toward the northeast. The estimated speed of the steady flow is greater than that expected for maximum flood-generated flow of tidal periodic flow. In this

https://doi.org/10.1017/S0016756897007450 Published online by Cambridge University Press

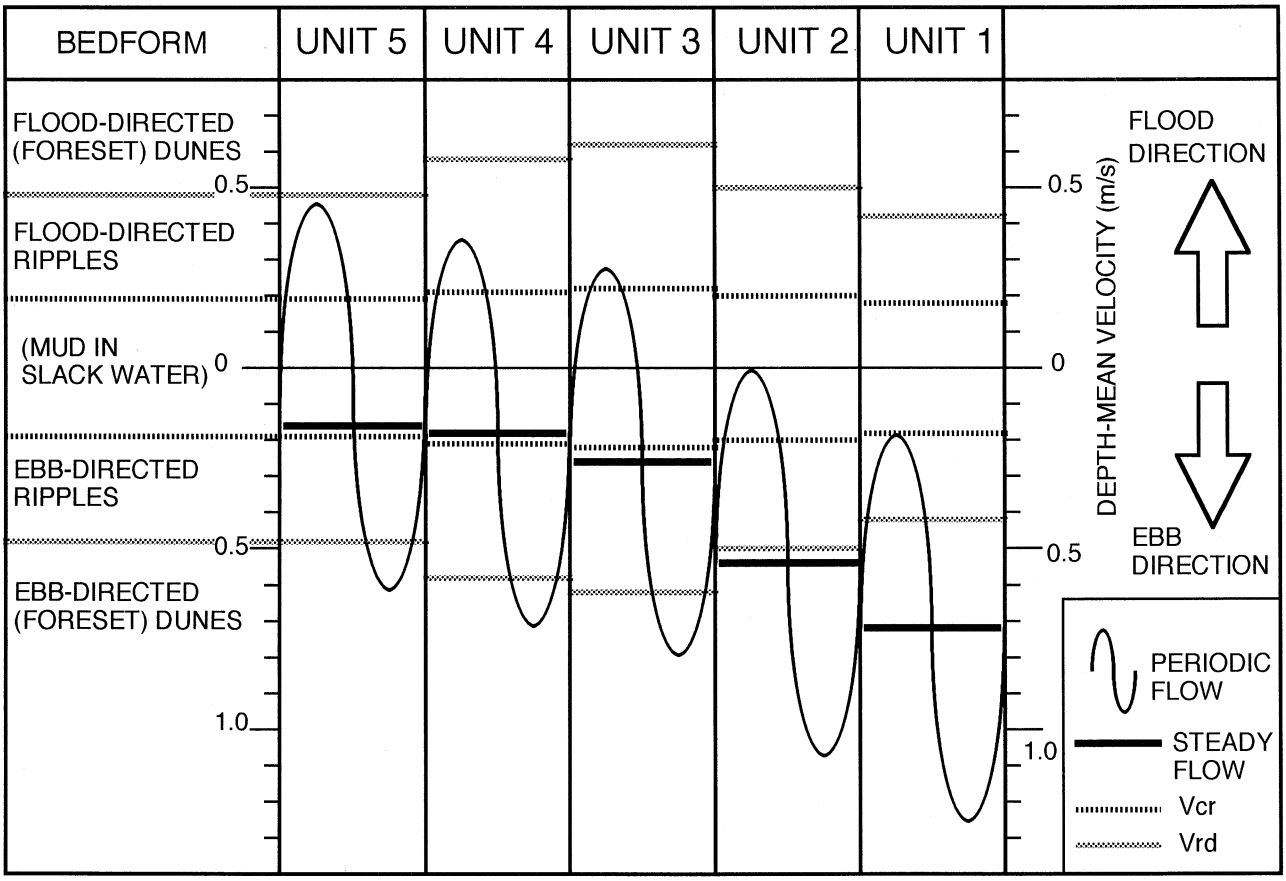


Figure 4. Summary of estimated velocity of periodic and steady flows for each unit. Depth-mean velocities for the threshold of sediment movement (Vcr), and ripple–dune transition (Vrd) calculated based on grain size and flow depth (Allen & Homewood, 1984). Dune–plane bed transition velocities (Vdpb) are not shown because the calculated velocities are almost the same as Vrd. Periodic flow curves are conceptional, and do not indicate neap–spring cycles. However, these curves are roughly consistent with the maximum velocity range during spring tide, which can be calculated from mud drape layer spacing.

way, the combined flows can form northeast-dipping dune foresets even during spring flood tide periods. Northeast-dipping dune foreset sandstones and mud drape layers of unit 2 are interpreted as deposits from slightly weaker steady flow, the speed of which was almost equal to that of the maximum flood-generated flow. Mud drape layers of unit 2 are deposited during slack water periods during flood tide periods. Bidirectional sandstone bedforms and mud drape layers of Units 3, 4 and 5 reflect well tidal periodic flow. The steady flow during these three units plays a part in forming asymmetric bedforms. Dune foreset sandstones are deposited during the ebb tide periods, while ripple sandstones are usually deposited during the flood tide periods. The superimposed subunit of unit 3 is exceptional and unique, and is suggestive of deposition from a flood-directed dominant current. This subunit may represent ephemeral and local deposits. It is often difficult to identify neap–spring cycles in these sandwave deposits, and the number of cycles forming each unit cannot be determined. The major reason for this is the starvation of sands which are insufficient to form tidal bundles (Allen, 1982), especially in units 4 and 5.

5. Palaeoflow velocities

Palaeoflow velocities in sediments can be estimated using grain size, bedform configuration, and flow depth (e.g. Allen, 1980, 1981; Nio, Siegenthaler & Yang, 1983; Allen & Homewood, 1984). From the occurrence of roots and recognition of a subtidal environment, flow depth is 3.0 m at the bottom of the thickest sandwave deposits (Nakayama *et al*. 1996). This depth is consistent with a range of 1 to 19 m assessed from bedform configuration (Allen & Homewood, 1984). Mean grain size of sandstones has been determined using a settling tube grain-size analyser (Tamura & Nakayama, 1993). Estimated palaeoflow depth-mean velocities for the threshold of sediment movement (Vcr), ripple–dune transition (Vrd), and dune–plane bed transition (Vdpb) are 0.18 to 0.22 m s^{-1}, 0.42 to 0.62 m s^{-1}, and 0.43 to 0.59 m s^{-1} respectively (Fig. 4). A periodic flow velocity range of 1.1 m s^{-1} can be estimated from unit 3. This range is the approximate maximum velocity range during spring tide, estimated by drape layer spacing in subunit of unit 3. Assuming this range is regular, the steady flow components are calculated as the difference between the mid point of periodic flow velocity and zero value (Fig. 4). The depth-mean velocities of ebb-directed steady flow thus gradually decrease from 0.72 to 0.16 m s^{-1} with progressive deposition. Almost all stratigraphic records of tidal sandwaves have been addressed to tidal cycles. The subtidal sandwave deposits described here are a rare instance in the stratigraphic record, which clearly suggest unidirectional to bidirectional bedforms influenced by gradually decreasing steady flow velocity.

Acknowledgements. I would like to sincerely thank to Dr B. P. Roser, and two anonymous reviewers for their comments on the manuscript.

https://doi.org/10.1017/S0016756897007450 Published online by Cambridge University Press

References

ALLEN, J. R. L. 1980. Sand waves: a model of origin and internal structure. *Sedimentary Geology* **26**, 281–328.

ALLEN, J. R. L. 1981. Palaeotidal speeds and ranges estimated from cross-bedding sets with mud drapes. *Nature* **293**, 394–6.

Allen, J. R. L. 1982. Simple models for the shape and symmetry of tidal sand waves: (1) statically stable equilibrium forms. *Marine Geology* **48**, 31–49.

ALLEN, P. A. & HOMEWOOD, P. 1984. Evolution and mechanics of a Miocene tidal sandwave. *Sedimentology* **31**, 63–81.

ASHLEY, G. M. 1990. Classification of large-scale subaqueous bedforms: a new look at an old problem. *Journal of Sedimentary Petrology* **60**, 160–72.

BERNER, R. A. 1984. Sedimentary pyrite formation: an update. *Geochimica et Cosmochimica Acta* **48**, 605–15.

COLEMAN, J. M. & WRIGHT, L. D. 1975. Modern river deltas: variability of processes and sand bodies. In *Deltas: Models for Exploration* (ed. M. L. Broussard), pp. 99–149. Houston: Houston Geological Society.

DALRYMPLE, R. W. 1984. Morphology and internal structure of sandwaves in the Bay of Fundy. *Sedimentology* **31**, 365–82.

DALRYMPLE, R. W., MAKINO, Y. & ZAITLIN, B. A. 1991. Temporal and spatial patterns of rhythmite deposition on mudflats in the macrotidal, Cobequid Bay–Salmon River estuary, Bay of Fundy, Canada. In *Clastic tidal sedimentology* (eds D. G. Smith, G. E. Reinson, B. A. Zaitlin and R. A. Rahmani), pp. 137–60. Canadian Society of Petroleum Geologist Memoir no. 16.

DE BOER, P. L., GELDER, A. VAN & NIO, S. D. (eds.) 1988. *Tide-influenced Sedimentary Environments and Facies*. Dordrecht: Reidel, 530 pp.

GASTALDO, R. A., ALLEN, G. R. & HUC, A. -Y. 1995. The tidal character of fluvial sediments of the modern Mahakam River delta, Kalimantan, Indonesia. In *Tidal Signatures in Modern and Ancient Sediments* (eds B. W. Flemming and A. Bartholoma), pp. 171–81. Special Publication of International Association of Sedimentologists no. 24.

HEDGES, J. I., CLARK, W. A. & COWIE, G. L. 1988. Organic matter sources to the water column and surficial sediments of a marine bay. *Limnology and Oceanography* **33**, 1116–36.

KANO, K. & NAKANO, S. 1985. Stratigraphic correlation of the Neogene in the San-in district, Southwest Japan, in the light of radiometric dating. *Bulletin of Geological Survey of Japan* **36**, 427–38 (in Japanese with English abstract).

KANO, K., YAMAUCHI, S., TAKAYASU, K. & MATSUMURA, H. 1994. *Geology of Matsue district with 1:50,000 Geological sheet*. Tsukuba: Geological Survey of Japan. 167 pp (in Japanese with English abstract).

MORRIS, P. A., ITAYA, T, WATANABE, T. & YAMAUCHI, S. 1990. Potassium/argon ages of Cenozoic igneous rocks from eastern Shimane Prefecture –Oki Dozen Island, Southwest Japan and the Japan Sea Opening. *Journal of Southeast Asia Earth Science* **4**, 125–31.

MURAKOSHI, N., NAKAYAMA, N. & MASUDA, F. 1995. Diurnal inequality pattern of the tide in the upper Pleistocene Paleo-Tokyo Bay: reconstruction from tidal deposits and growth-lines of fossil bivalves. In *Tidal Signatures in Modern and Ancient Sediments* (eds B. W. Flemming and A. Bartholoma), pp. 289–300. Special Publication of International Association of Sedimentologists no. 24.

NAKAYAMA, K., KAN, S., TAKAYASU, K. & SAMPEI, Y. 1996. Tidal sand waves in the Miocene Matsue Formation in Shimane Prefecture, Japan. *Journal of the Geological Society of Japan* **102**, 379–90 (in Japanese with English abstract).

NIO, S. D., SIEGENTHALER, C. & YANG, C. S. 1983. Megaripple cross-bedding as a tool for the reconstruction of paleohydraulics in Holocene subtidal environment, S. W. Netherland. *Geologie en Mijnbouw* **62**, 499–510.

REINECK, H. E. & WUNDERLICH, F. 1968. Classification and origin of flaser and lenticular bedding. *Sedimentology* **11**, 99–104 .

SUZUKI, T., TAKEDA, T. & KURIHARA, Y. 1988. Salt Marsh. In *Ecology and Ecothechnology in Estuarine-Coastal Area* (ed Y. Kurihara), pp. 142–9. Tokai University Press (in Japanese).

TAMURA, Y. & Nakayama, K. 1993. Guide for a grain-size analyzer with a settling tube system, and characteristics of its analysis. *Geological Report of Shimane University* **12**, 17–22 (in Japanese with English abstract).

VISSER, M. J. 1980. Neap–spring cycles reflected in Holocene subtidal large-scale bedform deposits: a preliminary note. *Geology* **8**, 543–6 .

WALKER, R. G. 1992. Facies, facies models and modern stratigraphic concepts. In *Facies Models: response to sea level change* (eds R. G. Walker and N. P. James), pp. 1–14. Ontario: Geological Association of Canada.

https://doi.org/10.1017/S0016756897007450 Published online by Cambridge University Press